JCIS Open 21 (2026) 100162

Contents lists available at ScienceDirect

JCIS Open

journal homepage: www.journals.elsevier.com/jcis-open

Permeation mechanism of gas molecules through polyimide barrier coatings with freeze- and oven-dried modified layered silicates

Joshua Lommes [a,b], Volkmar Stenzel [a], Andreas Hartwig [a,b,c,*]

[a] Fraunhofer Institute for Manufacturing Technology and Advanced Materials IFAM, Wiener Straße 12, Bremen, D-28359, Germany
[b] University of Bremen, Department 2 Biology/Chemistry, Leobener Straße 3, Bremen, D-28359, Germany
[c] University of Bremen, MAPEX Center for Materials and Processes, Bibliothekstraße 1, D-28359, Bremen, Germany

ARTICLE INFO

Keywords:
Layered silicates
Freeze dried
Activation energy
Organic modification
Barrier coating
Gas permeation

ABSTRACT

One effective strategy to improve the barrier performance of polymeric coating layers is the incorporation of layered silicate particles. This study investigates how the drying technology of silicates—specifically freeze-drying versus oven-drying—affects the permeation properties of the coatings. Modified layered silicates, prepared using both drying methods, are incorporated in varying amounts into polyimide coatings. The arrangement, orientation, and exfoliation of the particles are analysed using SEM. Results indicate that a higher proportion of layered silicates enhances the tortuosity of the diffusion pathway, thereby reducing permeability. Furthermore, permeation measurements of oxygen and water vapor, along with the calculated activation energies, reveal distinct differences in the permeation mechanisms of these gases through the coating films, highlighting the significant impact of the drying method on the barrier properties of the coatings.

1. Introduction

The permeation of gases through various materials is a critical topic across several application domains. Existing literature emphasizes the role of barriers in food packaging that not only prevent gas permeation but also mitigate the outgassing of intrinsic odours during storage [1]. Additionally, electronic devices, such as solar cells and high-power electronics, are encapsulated with barrier layers to prevent the ingress of moisture and oxygen, thereby reducing the risk of failure or oxidation of sensitive components [2,3]. In the context of mobility and energy applications, there is a growing demand for effective hydrogen storage and barrier properties against hydrogen permeation [4–6]. One potential application are coatings for carbon-fiber-reinforced polymer (CFRP) or glass-fiber-reinforced polymer (GFRP) tanks or pipes intended for hydrogen service, for example in aviation or automotive hydrogen fuel systems. Nonetheless, the focus of this work is on the activation energy of permeation for oxygen and water as examples which are especially important for packaging technology and electronic protection.

A well-established technique [1] to enhance the barrier properties of polymer coatings involves the incorporation of layered silicate or other layered particles, like graphene oxide, which also effectively reduce gas permeation [7–11]. This incorporation elongates the diffusion pathway, as detailed in the literature [12,13]. The tortuous paths created by the silicate particles extend the permeation route for gases through the polymer matrix, resulting in lower permeation coefficients [14]. A critical factor in achieving adequate barrier performance is the exfoliation and arrangement of the barrier particles within the polymer [15]. Prior studies have demonstrated that organic modification of the pigment surface facilitates delamination within the polymer coating, leading to improved barrier performance against gas permeation through the film [16–18]. Notably, the drying process significantly influences delamination and exfoliation characteristics. Freeze-dried modified layered silicates exhibit a superior degree of delamination compared to their oven-dried counterparts [14,16,18,19].

The primary objective of this study is to elucidate the gas permeation properties and mechanisms in relation to the drying process of the particles. This investigation compares freeze-dried modified layered silicates with oven-dried variants. Additionally, the influence of varying silicate proportions is examined to assess how particle quantity affects potential variations in permeation mechanisms.

Typically, a temperature increase of a system leads to enhanced permeation of substances through that system [20]. This temperature effect results from the cumulative impact of various processes occurring during permeation. As temperature increases, the solubility of gases or

* Corresponding author. Fraunhofer Institute for Manufacturing Technology and Advanced Materials IFAM, Wiener Straße 12, Bremen, D-28359, Germany.
E-mail address: andreas.hartwig@ifam.fraunhofer.de (A. Hartwig).

https://doi.org/10.1016/j.jciso.2025.100162
Received 5 August 2025; Received in revised form 11 November 2025; Accepted 17 November 2025
Available online 19 November 2025

volatile compounds in a polymer generally decreases. However, the increase in diffusion rates is usually significantly larger, rendering diffusion the rate-limiting step in the overall process. Previous studies have primarily focused on systems with lower filler concentrations, typically up to 5 %, with a maximum of 10 % [1,8]. It is hypothesized that higher concentrations of modified particles can effectively reduce permeation rates. Notably, the advantages of freeze-dried and organically modified phyllosilicates present opportunities for achieving a substantially higher degree of filling.

2. Materials and methods

2.1. Materials

Layered silicates Cloisite Na+ (CNa+) and the dispersing agent Anti-Terra 203 were obtained from BYK Additives and Instruments (Wesel, Germany). The polyimide P84® was purchased from Ensinger GmbH (Nufringen, Germany). Hydrochloric acid (HCl) (37 %), *N,N*-dimethylacetamide (DMAc) (99.8 %, anhydrous) and dodecylamine (DDA) (98 %) were supplied from Merk (Darmstadt, Germany).

Water Vapor permeation (WVP) and oxygen permeation coefficient (OPC) measurements were performed on PET films PetroPET 406 with a thickness of 23 µm from Petroplast (Neuss, Germany). The PET foil is a high temperature resistant foil, with high permeability to prevent an influence on the permeation of the coatings.

2.2. Methods

2.2.1. Synthesis of organically modified silicates

The synthesis of the silicates was carried out following our previous work [14]. Layered silicates were modified with dodecylamine in a two-step process. First, 5 g of the layered silicate Cloisite Na+ was exfoliated in 200 mL of deionized water at 80 °C for 1 h. A second solution was prepared by mixing 100 mL of deionized water, 2.22 g of dodecylamine, and 1.31 g of hydrochloric acid to protonate the amine, which was also stirred for 1 h. After combining these two dispersions, the modified particles were filtered and dried. For oven drying the silicates were dried at 60 °C for 72 h. Freeze drying was performed at –18 °C at 0.1 mbar for 72 h. The exchange reaction has already been investigated in previous work. XPS measurements show the completely exchanged sodium ion and the fully protonated nitrogen [16].

2.2.2. Formulation, application and curing of barrier coatings

According to previous work, the formulation, application and curing of the barrier coatings were performed [14,16]. The granulated polyimide P84® was dissolved in dimethylacetamide for 12 h, resulting in a 25 wt% solution. For the second solution, modified layered silicate was dispersed in the solvent with a weight content of 5 wt% particles. The solvent, silicate particles and 1 wt% (based on total mass) dispersing agent Anti-Terra 203 were mixed and dispersed at 2200 min^{-1} using a Dispermat® from VMA-Getzmann (Reichsdorf, Germany).

Both solutions were combined in different ratios. Finally, all formulations listed in Table 1, were dispersed at 2000 min^{-1}. After dispersing, the coatings were defoamed with a SpeedMixer® from Hauschild (Hamm, Germany). This process was performed for both oven dried layered silicates and freeze-dried particles, achieving the particle contents of 10, 30 and 60 wt% in the dry coating layers. The high concentration was possible due to a combination of the solvent, the dispersing agent and the preparation of these coatings.

Barrier coatings were applied using a film applicator from TQC Sheen (Hilden, Germany). For the permeation measurements, the films were applied on PET substrates, while SEM measurements were conducted on aluminium substrates from Q-Lab (Westlake, USA). The wet film thickness on all substrates was 200 µm resulting in a dry thickness of about 5–20 µm, as predicted. The viscosities of all coatings used were within a range that allows the problem-free processing during the formulation, application and curing.

Table 1
Composition of barrier coatings with various content of modified layered silicates (oven and freeze-dried).

Barrier-Coating	–1	–2	–3	–4	–5	–6
Substance	[g]	[g]	[g]	[g]	[g]	[g]
Freeze-dried modified silicate 5 % in DMAc	34.5	67.0	87.5	–	–	–
Oven-dried modified silicate 5 % in DMAc	–	–	–	34.5	67.0	87.5
P84® in DMAc (25 %) + Anti Terra 203	65.5	33.0	12.5	65.5	33.0	12.5
Sum	100	100	100	100	100	100
wt% silicate in dried films	10	30	60	10	30	60

Curing of the films was done in three steps. First, the films were physically dried at room temperature for 10 min before cured for 5 min with UV-radiation. This also promotes the alignment of the silicates through volume shrinkage. The mercury lamps intensity was 0.08 W cm^{-1}. Finally, the coatings were cured 20 min in an oven at 150 °C. This enables the system to be completely fixed and cured and is a decisive factor in its adhesion to the substrate.

2.2.3. Characterization

The different orientation, degree of delamination/exfoliation and the arrangement of the layered silicates in the barrier coatings were investigated using scanning electron microscopy (SEM). The samples were prepared by cutting them into small specimens and embedded into Spurr epoxy resin. The resin was hardened for 12 h at 70 °C. With an Ultra Microtome Leica UltraCut CC, the samples were cut into cross sections. Electrical charging was prevented by vapor-coating of the resulting cross sections with carbon layers of 5–10 nm thickness. The SEM images were obtained with a FEI Helios Nano Lab 600 (DualBeam) from Thermo Fischer Scientific. For each coating five SEM images were performed from different points over the whole extension of the sample to verify the particle distribution through the sample.

To determine the performance of the barrier coatings and calculate the activation energies, the permeation of water vapor and oxygen was measured according to ASTM D3985, ASTM F1249 and ISO 15106–2. A C406H permeation tester from Labthink (Neu-Isenburg, Germany) was used to determine the permeation coefficients. For permeation measurements film thicknesses were measured from each sample. The measuring device automatically performs a leak test to ensure that the cell and coating are leak-proof. Nitrogen with a purity >99.95 % was used as feeding gas. The oxygen permeation measurement was performed at 0 % relative humidity, while the water vapor permeation was determined at 90 % relative humidity. The measurements were performed at several temperatures (288 K; 293 K; 298 K; 303 K; 313 K and 323 K). All measurements were performed in triplicate. Each measurement was repeated until three consecutive values were consistent.

The relative humidity was maintained constant across all investigated temperatures. This means that the absolute humidity increases with increasing temperature. Previous studies have shown that permeation is primarily influenced by the water uptake of the polyimide and saturation is obtained already at low humidities [21]. This is due to interaction of the water with the imide groups as distinct adsorption sites. To ensure that all sites are blocked, and the water amount can be taken constant independently on the absolute humidity the relative humidity was set to 90 %. The water saturation of polyimides are in the range of a few percent [22].

For low temperature measurements, the permeation of gases can be easily determined from the flux (F_{gas}), the specimen thickness (substrate + coating) (d), and the partial pressure (p_{gas}) of the measured gas. This relationship leads to equation (1), where the permeation of a gas can be calculated.

$$Perm_{gas} = \frac{F_{gas} \cdot d}{p_{gas}} \quad (1)$$

From these results, the activation energy of the permeation can be calculated by plotting the permeation coefficients against the inverse temperature. The slope of the resulting Arrhenius plots indicates the activation energy for the permeation of the investigated gas through the barrier coating [4,23].

To determine a glass transition temperature of the coatings modulated differential scanning calorimetry (MDSC) were performed with the coating systems in Table 1. For this, a small amount (3–10 mg) of each coating were weight into the Discovery DSC from TA Instruments (Hüllhorst, Germany). The investigated temperature range was set from −50 °C to 300 °C with a heating rate of 3 K min^{-1}, an amplitude of 1 K min^{-1} and a frequency 60 s^{-1}.

3. Results and discussion

3.1. SEM images and mechanical properties

To investigate the orientation and exfoliation of the platelike particles, SEM images were obtained from all barrier coatings. Two particle types, resulting from the oven-drying and the freeze-drying processes, were compared based on their arrangement, orientation, and exfoliation state. It is expected that a higher silicate content is clearly visible in the SEM images. Furthermore, it is postulated that the freeze-dried layered silicates show improved exfoliation compared to the oven-dried particles.

Fig. 1 a) shows the SEM images of the barrier coatings with 10 % silicate particles at a magnification of 4000. The silicate particles are visible in the barrier coating as light grey to white fragments in the dark polyimide film. The arrangement of the pigments from both drying types

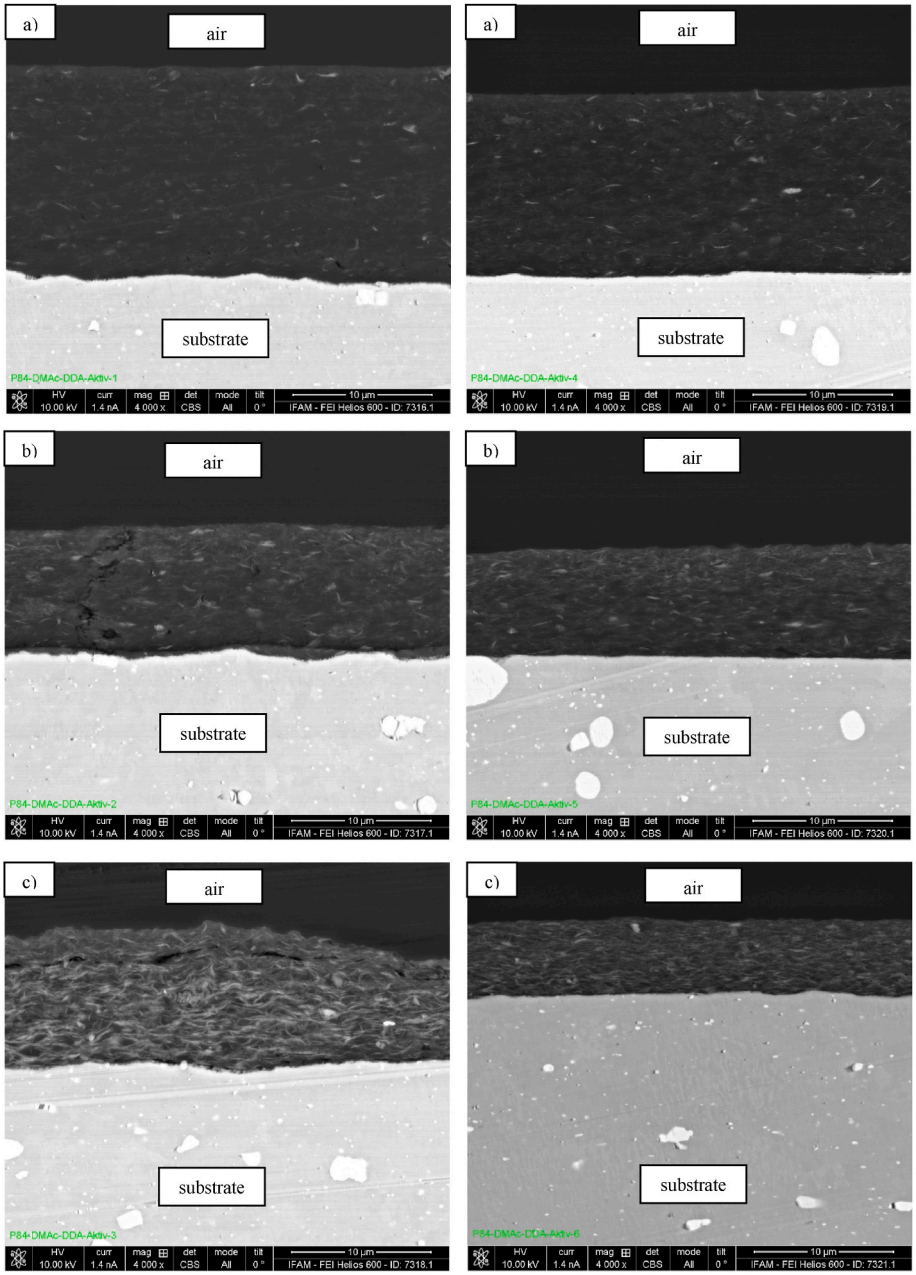

Fig. 1. SEM images of barrier coatings with freeze- (left) and oven-dried (right) particles at a) 10 wt%, b) 30 wt% and c) 60 wt% of modified layered silicates at a magnification of 4000.

is homogeneous throughout both films. Nevertheless, the amount of the polymer free volume is very high between the particles, allowing many diffusion paths for gases to permeate through the coating layer.

Fig. 1 b) shows the SEM image of coatings with 30 % silicate content with a magnification of 4000. The higher number of particles is clearly visible compared to the lower silicate content in Fig. 1a). Furthermore, the freeze-dried particles in coating 2 are stronger aligned in the film. However, the freeze-dried particles also show an improved delamination and better orientation in the coatings compared to coatings with lower particle content as well as compared to oven-dried ones.

For the oven-dried particles in coating 5, a higher concentration of particles is also visible at the interface between the coating and air. The exfoliation of some particles can be observed as well. However, stronger agglomeration of layered silicate can be seen in the coating. The layered silicate particles are not delaminated and exfoliated in these agglomerates. Therefore, a lower number of particles can form a barrier against gas diffusion.

In summary of the SEM examinations, it seems that the amount, orientation, and arrangement of particles influence the barrier formation. A lower gas permeation is postulated for these barrier coatings with high particle amount compared to ones with lower pigment content. From the images it is furthermore postulated that the freeze-dried particles form a higher barrier against gas permeation in contrast to the oven-dried particles as they are stronger exfoliated and better distributed.

In addition, the interphase content increases with higher particle amount. This was shown by SEM and TEM image evaluation in our previous work [17]. The SEM images presented here also show an increase of the coating's silicate content. However, an increase of the silicate amount does not automatically mean an increase of the interphase as this also depends on the intercalation and exfoliation of the particles.

The images shown here, together with the TEM images from Ref. [17], indicate intercalation and especially also for the coatings with low particle amount also exfoliation of the particles. This shows that the interphase fraction increases with increasing particle content but at very high particle content it might go back due to decreasing polymer amount and impossibility of proper exfoliation. A rise in interphase content increases the potential permeation through the interphases compared to the polymer not influenced by the particles. Therefore, the permeants might migrate through the polymer or through the interphases and should be blocked by the particles.

Consistent with our previous studies, the incorporation of layered silicates exerts only a small influence on the mechanical properties of the coatings. Adhesion to the substrate, as assessed by the cross-cut test, remains unchanged for coatings with or without silicates. The crosscut value is for coatings with and without layered silicates zero. The only noticeable deviation is a reduction in pendulum hardness with the addition of layered silicates from 146 counts (without silicates) to 102 counts (with silicates). Nevertheless, the coatings maintain excellent adhesion to the substrate, and their hardness remains sufficient for subsequent applications [18].

Fig. 1 c) shows SEM images of the coatings with the highest content of layered silicates (60 %). The particles are clearly visible in the coating with a homogenous distribution and a horizontal arrangement of the flakes. In coating 3, which contains freeze-dried layered silicates, delaminated and partially exfoliated particles can be observed. It is assumed that the higher number of particles, along their orientation, arrangement, and the higher degree of delamination and exfoliation in coating 3, leads to lower gas permeation compared to coatings with lower particle contents.

In contrast, the oven-dried particles in coating 6 exhibit slightly different appearance. Here, a high number of particles are orientated parallel to the surface, similar to the freeze-dried modified layered silicates. The particle arrangement in the coatings is not significantly different between the two drying methods. However, coating 6 shows some particle agglomerates. Furthermore, delamination does not take place to the same extent compared to coating 3.

The particles in coating 3 are brighter, and their edging is slightly blurred. In contrast, coatings 6 displays sharp outlines of the particles. The oven-dried particles are not delaminated or exfoliated to the same degree as the freeze-dried modified layered silicates. These findings confirm previous results, namely that freeze-dried silicates have a larger particle layer spacing leading to an improved delamination. This has already been published and was investigated using XRD, BET, SEM, and TEM [18].

The different concentration of layered silicates can be clearly distinguished by SEM. Furthermore, with an increased pigment concentration, the orientation, arrangement, and degree of delamination and exfoliation improve. It is postulated that a higher barrier pigment concentration will lead to improved barrier properties of the film. Additionally, the freeze-dried particles show stronger orientation and a higher degree of delamination/exfoliation as described in previous work [18]. Therefore, the permeation values of coatings 1–3 are postulated to be lower compared to the coatings 4–6, despite having equal pigment concentrations with oven-dried particles.

3.2. Modulated DSC

Modulated DSC measurements from coatings without particles as well as with 60 wt% freeze and oven dried particles, shown in Fig. 2, are indicating no glass transition over the investigated temperature range of −50 to 300 °C. The blue curves are showing the reversing heat flow. A glass transition would be detected by a step. A glass transition is expected in the examined temperature range, most likely if expands over a wide temperature range due to non-uniformity of the polymer and is therefore below the detection limit of the temperature.

The observed peaks in the non-reversible heat flow indicate a post-curing reaction, which typically occurs at temperatures starting from the previous curing temperature.

A potential glass transition would have a pronounced impact on the permeation behaviour. The glass transition would substantially alter the properties of the polymer in the coating, thereby complicating the ability to draw conclusions about any potential differences in the permeation mechanisms across the investigated temperature range. The absence of an observable glass transition implies that any potential influences of this phenomenon can be excluded from the subsequent discussion. Therefore, the permeations can be directly compared in terms of their behaviour, independent of the temperature under investigation.

TGA did not show weight losses at temperatures similar to the irreversible peaks observed by MDSC. From this we conclude that they are not caused by a weight loss but a post-curing.

3.3. Oxygen permeation

To verify the postulates regarding permeation behaviour derived from the SEM images, permeation measurements were performed at different temperatures.

Fig. 3 shows the Arrhenius plot of the logarithmic oxygen permeation coefficients (OPC) in dependence on the reciprocal temperature. For the coatings with freeze-dried layered silicates higher concentrations of particles lead to a lower OPC. The OPC increases with increasing temperature. Coating 1 (10 % silicate) shows an oxygen permeation coefficient of $3.6{\cdot}10^{-12}$ cm^3 cm $cm^{-2}{\cdot}s^{-1}{\cdot}cmHg^{-1}$ at 15 °C and an increased OPC of $1.6{\cdot}10^{-11}$ cm^3 cm $cm^{-2}{\cdot}s^{-1}{\cdot}cmHg^{-1}$ at 50 °C. This trend can be observed for all coatings. Coatings without particles show a significantly higher permeation (one to two orders of magnitude) at all temperatures.

The coatings with oven-dried layered silicates also show a decrease of the OPC with higher particle concentration. Furthermore, the temperature has the same influence. The OPC increases starting from $3.9{\cdot}10^{-12}$ cm^3 cm $cm^{-2}{\cdot}s^{-1}{\cdot}cmHg^{-1}$ at 15 °C to $20.8{\cdot}10^{-12}$ cm^3 cm $cm^{-2}{\cdot}s^{-1}{\cdot}cmHg^{-1}$ at 50 °C for coating 4 (10 % silicate).

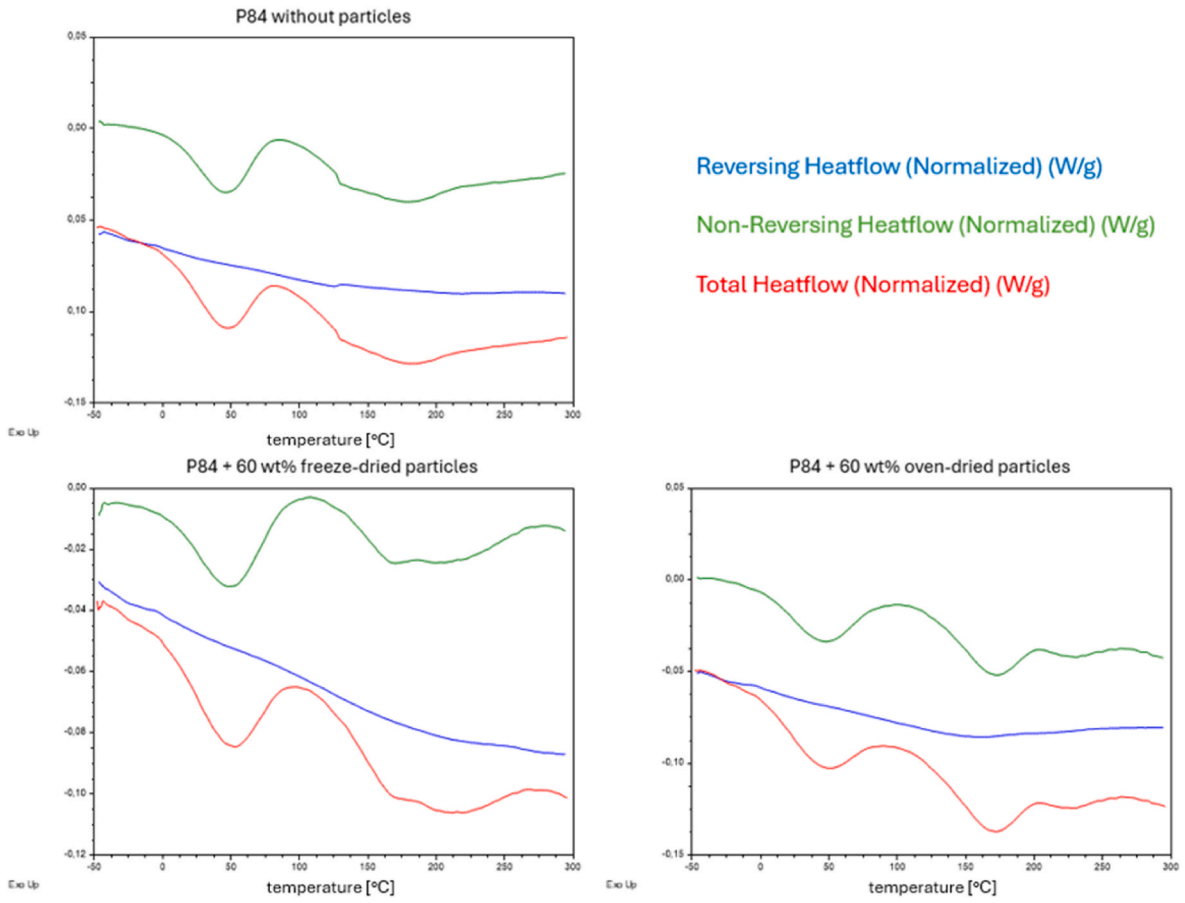

Fig. 2. MDSC curves of barrier coatings without particles (top) and with 60 % of freeze dried (bottom left) and 60 % oven dried (bottom right) layered silicates.

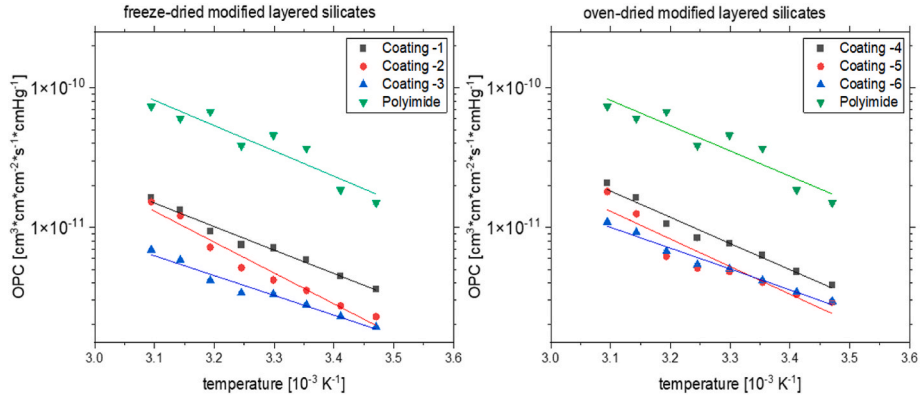

Fig. 3. Oxygen permeation coefficients in dependence of the temperature (Arrhenius plot) for freeze-dried (left) and oven-dried (right) layered silicates compared to polyimide coatings without particles.

Comparing the two differently dried types of silicates, it is observed that the freeze dried layered silicate leads to a higher barrier against the permeation of oxygen through the polyimide coating. All these results agree with the postulate drawn after analysing the SEM images regarding the barrier properties of these coatings. Compared to literature OPC of pure polyimide (Kapton), barrier property was improved by a factor ten at ambient temperature [23,24].

With higher temperature, the dynamic of the polymers free volume increases as well as the diffusion through the polymeric film. The solubility of the gas decreases with increasing temperature [25,26]. However, the increase in diffusion is higher than the solubility decreases, resulting in an overall increase in OPC with increasing temperature. This trend can be observed for all coatings independent on the drying process of the barrier pigments. In addition, the slope of the lines is similar for all examined coatings indicating similar activation energies for oxygen permeation.

The relationship between permeation (P) can be expressed as a function $P = S \cdot D$ of solubility (S) and diffusion (D). Based on this equation, the observed phenomenon can be mathematically represented when absorption and desorption of the gases are neglected. The permeation, which is constituted in this manner, is thus influenced by temperature. As the temperature increases, diffusion rises due to the enhanced mobility of the polymer and the permeate. On the other hand, there is a decrease in the solubility of the permeate in the polymer.

3.4. Water vapor permeation

Temperature dependence of water vapor permeation (WVP) was also measured for the coatings, and the results show a different behaviour compared to the OPC. Fig. 4 shows the logarithmic WVP in dependence on the reciprocal temperature (Arrhenius plot). Similar to the OPC, the WVP decreased with increasing amount of silicate particles in the coatings. For coatings with the lowest barrier pigment content, the WVP decreases with increasing temperature. Coating 1, with 10 % of freeze-dried particles, shows a WVP of $4.0{\cdot}10^{-14}$ g cm $cm^{-2}{\cdot}s^{-1}$ Pa^{-1} at 15 °C. At higher temperature (50 °C), the permeation decreases to $2.8{\cdot}10^{-14}$ g cm $cm^{-2}{\cdot}s^{-1}$ Pa^{-1}. Coating 4, with 10 % oven dried layered silicate, exhibits similar behaviour, with the WVP decreasing from $5.5{\cdot}10^{-14}$ g cm $cm^{-2}{\cdot}s^{-1}$ Pa^{-1} at 15 °C to $3.5{\cdot}10^{-14}$ g cm $cm^{-2}{\cdot}s^{-1}$ Pa^{-1} at 50 °C.

At higher silicate contents, the WVP decreases with increasing temperature. For coatings with 60 % pigments, the WVP rises from $7.4{\cdot}10^{-15}$ g cm $cm^{-2}{\cdot}s^{-1}$ Pa^{-1} at 15 °C to $1.1{\cdot}10^{-14}$ g cm $cm^{-2}{\cdot}s^{-1}$ Pa^{-1} at 50 °C for freeze-dried silicates, and $8.7{\cdot}10^{-15}$ g cm $cm^{-2}{\cdot}s^{-1}$ Pa^{-1} at 15 °C to $0.17{\cdot}10^{-15}$ g cm $cm^{-2}{\cdot}s^{-1}$ Pa^{-1} at 50 °C for oven-dried silicates. For coatings with 30 % silicate, the WVP remains nearly constant with increasing temperature. As observed for OPC, coatings without particles show a permeation, which is one to two orders of magnitude higher compared with coatings containing particles. In addition, permeation almost does not depend on the temperature.

The relative humidity chosen here was maintained constant over the measured temperature range. This results in a change in absolute humidity with varying temperature. However, as already demonstrated in the literature, this does not have any impact on permeation. This independence is due to the water adsorption at the imide sites which are already saturated at low humidities. Therefore, the water concentration can be taken constant [21].

This is also verified by our measurement of the polyimide coating without particles. The permeation does not change by varying the temperature and with this by the change in absolute humidity.

Like OPC, the WPC decreases with increasing pigment content in the coatings. Furthermore, freeze-dried layered silicates exhibit lower WVP compared to oven-dried particles, which was postulated from SEM images. The WVP of polyimide (Kapton®) in the literature is $2.7{\cdot}10^{-14}$ g cm $cm^{-2}{\cdot}s^{-1}$ Pa^{-1} at 30 °C which is lower than the value of $1.3{\cdot}10^{-13}$ g cm $cm^{-2}{\cdot}s^{-1}$ Pa^{-1} obtained by us [27]. This is most likely due to the not identical composition and our two step drying process which does not lead to an ideal structure as that from Kapton®. Nevertheless, even in comparison with the ideally structures Kapton® we obtain an improvement by a factor of 3. This is with the two coating with freeze-dried particles at a concentration of 60 % resulting in a permeation of $0.89{\cdot}10^{-14}$ g cm $cm^{-2}{\cdot}s^{-1}$ Pa^{-1}. In general, the slopes of the lines are similar for all coatings and is close to zero. This indicates similar and small activation energies for water transport for all coatings.

OPC and WVP show different behavior with increasing temperature. As discussed earlier, the OPC increases with rising temperature due to the higher oxygen mobility and higher polymer mobility. The WVP, however, only increases slightly with a higher concentration of silicate particles in the coating. For lower concentration, the WVP decreases with increasing temperature, and at medium concentration of particles, the WVP shows no significant changes with temperature increase. Water is a polar molecule. Water molecules can be absorbed by the layered silicate particles along the permeation direction. In addition to the absorption of water vapor molecules, hydrogen bonds can be formed with the polymer, thereby significantly influencing the diffusion through the layer. This phenomenon is well-documented in the literature and is referred to as the "polar tortuous path." This model is applicable to polar substances, whereas the permeation of nonpolar substances is predominantly governed by tortuosity [4,13,28]. Furthermore, the possible formation of interphases between the particle surface and the polymer occurs. With an increasing number of particles, the amount of interphase also increases. Diffusion of polar water molecules might occur in the interphase between the layered silicates and the polyimide.

At lower particle concentration the distances between the particles are notably larger. Therefore, permeation through the layer is minimally affected. However, when the silicate content in the coating increases, the influence of the polar tortuous path becomes more pronounced. Permeation is impacted by the enhanced absorption of water molecules by the silicates in the phases and the formation of hydrogen bonds with the polymer. In combination with the reduced amount of dissolved water in the polymer, an increase in the silicate concentration (30 %, 60 %) leads to a reduction in permeation with rising temperature. In contrast, coatings containing only 10 % modified layered silicates exhibit an increase in permeation with rising temperature, a behaviour also observed with oxygen. This phenomenon is independent of the drying method used for the silicates.

3.5. Activation energies of permeation

From the permeation data and the logarithmic presentation in the diagrams, the activation energies (E_A) for permeation can be calculated as the slope (A_e) of the linear temperature-dependent permeation values for both gases by using the Arrhenius equation $\ln P = \ln A_e{\cdot}\frac{E_A}{RT}$. Fig. 5 shows the calculated activation energies for oxygen permeation through the barrier coatings with different pigment concentrations of freeze-dried and oven-dried modified layered silicates.

For oxygen permeation, all activation energies are positive, indicating that the permeation of oxygen through these barrier coatings requires energy to initiate and sustain permeation. The higher the activation energy, the more energy is needed to initiate the transport. A higher activation energy is desirable for barrier coatings. The barrier coatings with freeze-dried silicates have an activation energy of 32.2 kJ mol^{-1} for 10 % particle concentration, 42.3 kJ mol^{-1} for 30 % and 27.1

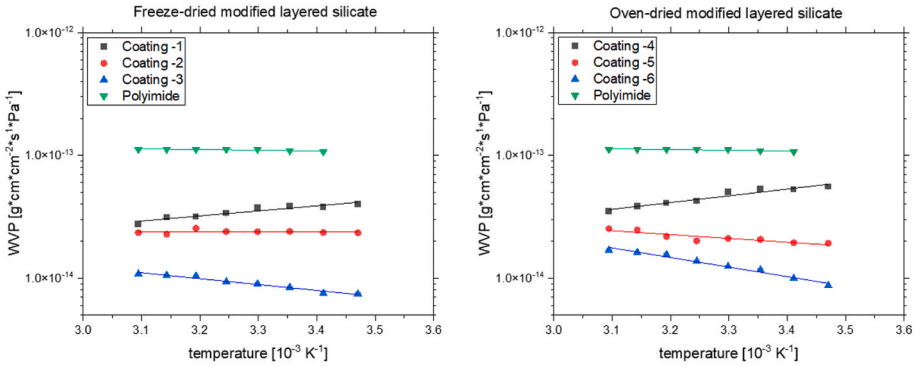

Fig. 4. Water vapor permeation coefficients in dependence of the temperature for coatings with different amount of freeze-dried (left) and oven-dried (right) layered silicates compared to polyimide coatings without particles.

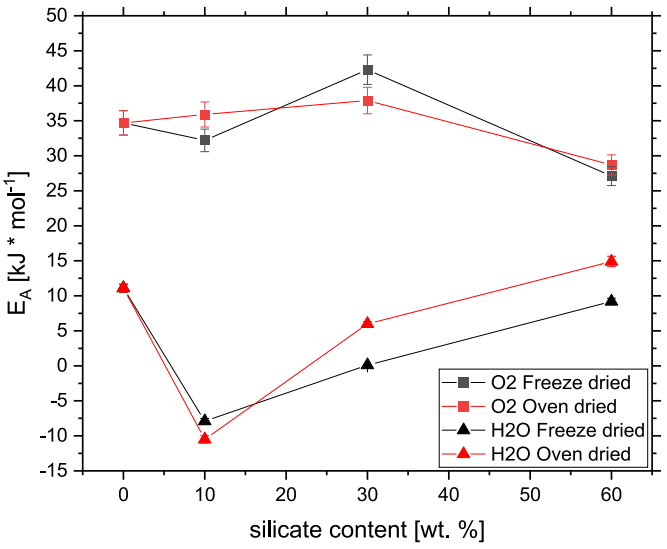

Fig. 5. Calculated activation energies for oxygen and water vapor permeation through polyimide coatings with different amount of freeze-dried and oven-dried layered silicates (the points are connected as guide for the eyes).

kJ mol^{-1} for 60 %, respectively. For coatings with oven-dried layered particles, the E_A were calculated as 35.9 kJ mol^{-1} for 10 % particle concentration, 37.9 kJ mol^{-1} for 30 % and 28.7 kJ mol^{-1} for the coating with a particle concentration of 60 %. The coating without silicates has a calculated activation energy of 34.7 kJ mol^{-1}.

Firstly, the E_A for oxygen permeation tend to increase, with an increasing number of particles within the coating. Secondly, for a silicate content of 60 wt%, the lowest activation energies were calculated, indicating that oxygen permeation occurs more spontaneously and readily. By introducing additional particles, permeation seem to take place by an additional mechanism. The diffusion of oxygen molecules occurs not only through the tortuous path and through the polymer but also migrates more easily and rapidly along the phase boundaries between the particles and the polymer [4,29]. In addition, a high particle load might lead to defects in the coating on microscopic scale. A higher proportion of particles results in a larger number of possible diffusion paths, thereby reducing the activation energy. The extent to which these paths are utilized depends on the number of particles, temperature, gas solubility, and the polarity difference between polymer and the gas, as well as between the gas and the particles interphases. Non-polar gases, such as oxygen, interact minimally with the polymer and might prefer to diffuse through the interphase.

From the SEM and TEM data, the number of interphases increases with higher silicate content. Without silicate permeation occurs only through the polymer, at 30 wt% silicate already the particles can still orient, and a medium amount of interphase is available leading to an increase of activation energy. If the silicate amount increases further (60 wt%) the quality of orientation and exfoliation decreases, and probably microscopic defects are formed. Together with the increasing interphase content this leads to the observed decrease of activation energy for oxygen permeation for composites with very high particle amounts.

The activation energies for water vapor permeation (WVP) through the coatings were calculated and are also shown in Fig. 5. These values differ from those for oxygen permeation as they are smaller and close to zero and go through a minimum with negative values. The coatings with 10 wt% layered silicate exhibit negative activation energies of −7.9 kJ mol^{-1} for freeze-dried and −10.5 kJ mol^{-1} for oven-dried particles, respectively, indicating a spontaneous and readily occurring permeation process. As the particle concentration increases, the activation energies become positive, reaching 9.2 kJ mol^{-1} (freeze-dried) and 14.9 kJ mol^{-1} (oven-dried) at 60 wt% silicate.

Due to the formation of hydrogen bridges between the polar PI and water molecules the affinity between both is higher compared to oxygen leading to the observed lower activation energy for permeation. The activation energy's minimum at 10 wt% silicate might be explained by formation of the polar interphases containing ionic compounds. They seem to dominate the water transport at low particle amounts. With further increasing silicate amount the content of the polar polymer decreases and the permeation blocking effect of the particles becomes more dominant. These effects together are an explanation for the increasing activation energies for particle amounts exceeding 10 wt%.

4. Conclusions

This study aimed to investigate the influence of the drying process of organically modified montmorillonite on gas permeation through polymer films. Especially oxygen and water permeations were examined for the purpose of packaging and electronic applications. Factors examined include the delamination of particles within the polymer, the arrangement of barrier pigments in the matrix, tortuosity, particle proportion, and the resulting permeation coefficients, as well as the activation energy of permeation.

The results indicate that freeze-dried modified layered silicates exhibit a higher degree of delamination and exfoliation compared to oven-dried modified layered silicates, as evidenced by Scanning Electron Microscopy (SEM). These findings corroborate previous work, which demonstrated that freeze-dried layered silicates show greater delamination based on layer spacing measurements obtained from X-ray diffraction (XRD) [18]. A higher filling degree of particles in the polymer leads to a more pronounced tortuous path but might also result in microscopic defects.

Permeation coefficients were determined, revealing reduced permeation of both gases with increasing concentrations of barrier pigments. Notably, freeze-dried layered silicates consistently demonstrated lower permeation coefficients for oxygen and water vapor across all investigated silicate contents. The type of drying applied to the barrier pigments significantly influences both the exfoliation of the particles and the gas permeation through coatings filled with these pigments.

Temperature increases resulted in enhanced permeation for oxygen, while the permeation of water vapor decreased with rising temperature at 10 % silicate content. However, at higher particle concentrations (60 % silicate), an increase in temperature led to higher permeation of water vapor, indicating different permeation mechanisms for the two gases.

The activation energies further confirm different permeation behaviour for oxygen and water vapor. For oxygen, activation energies increase with silicate content from 10 % to 30 %, then decrease to a minimum at 60 % silicate, a trend observed for both freeze-dried and oven-dried particles. Oxygen permeates not only through the polymers free volume but also at the silicate-polymer interface, where higher particle content increases the boundary area, facilitating permeation. In contrast water interacts with the polar polyimide so that the permeation activation energy is lower than for oxygen. At low silicate contents (10 wt%) water vapor permeation exhibits negative activation energies, where interactions between the polar interphases and polar water promote spontaneous permeation. At higher silicate contents, increased tortuosity hinders permeation leading to the observed increase of the activation energies.

These findings highlight the different permeation mechanisms of gases and their implications for optimizing barrier coatings. By modifying layered silicates in an appropriate way, development of coatings with enhanced gas resistance for various applications are improved. Additionally, the study emphasizes the crucial impact of the freeze-drying process on the performance of these modified layered silicates as barrier pigment.

CRediT authorship contribution statement

Joshua Lommes: Writing – original draft, Visualization, Methodology, Investigation, Data curation, Conceptualization. **Volkmar Stenzel:** Writing – review & editing, Supervision, Resources, Project administration, Funding acquisition. **Andreas Hartwig:** Writing – review & editing, Validation, Supervision, Conceptualization.

Declaration of competing interest

The authors declare that they have no known competing financial interests or personal relationships that could have appeared to influence the work reported in this paper.

Acknowledgements

The funding of this investigation within the LUFO project HYTANK (FKZ: 20W2214D) by the German Federal Ministry for Economic Affairs and Climate Action (BMWK) is gratefully acknowledged. The authors would also like to acknowledge Karsten Thiel, and Jonas Aniol for the preparation and execution of SEM analyses, as well as Katja Marnitz for MDSC measurements.

Appendix A. Supplementary data

Supplementary data to this article can be found online at https://doi.org/10.1016/j.jciso.2025.100162.

Data availability

Data will be made available on request.

References

[1] A. Arora, G.W. Padua, Review: nanocomposites in food packaging, J. Food Sci. 75 (2010), https://doi.org/10.1111/j.1750-3841.2009.01456.x. John Wiley & Sons, Ltd, https://ift.onlinelibrary.wiley.com/doi/10.1111/j.1750-3841.2009.01456.x.
[2] M. Manceau, A. Rivaton, J.-L. Gardette, S. Guillerez, N. Lemaître, The mechanism of photo- and thermooxidation of poly(3-hexylthiophene) (P3HT) reconsidered, Polym. Degrad. Stabil. 94 (2009), https://doi.org/10.1016/j.polymdegradstab.2009.03.005. https://www.sciencedirect.com/science/article/pii/S0141391009000883.
[3] M. Hanf, J.-H. Peters, S. Clausner, N. Kaminski, Hydrogen sulphide (H2S) single gas testing on power semiconductor modules under high voltage, Microelectron. Reliab. 138 (2022), https://doi.org/10.1016/j.microrel.2022.114622. Elsevier BV.
[4] S. Schiessl, E. Kucukpinar, R. Schwiddessen, H.-C. Langowski, P. Eisner, Mechanisms of permeation of helium, hydrogen, oxygen, and water vapor through silicate-based composite barrier coating layers, Surf. Coating. Technol. 483 (2024), https://doi.org/10.1016/j.surfcoat.2024.130800. https://www.sciencedirect.com/science/article/pii/S0257897224004316.
[5] B. Sezgin, Y. Devrim, T. Ozturk, I. Eroglu, Hydrogen energy systems for underwater applications, Int. J. Hydrogen Energy 47 (2022), https://doi.org/10.1016/j.ijhydene.2022.01.192.
[6] A. Escamilla, D. Sánchez, L. García-Rodríguez, Assessment of power-to-power renewable energy storage based on the smart integration of hydrogen and micro gas turbine technologies, Int. J. Hydrogen Energy 47 (2022), https://doi.org/10.1016/j.ijhydene.2022.03.238.
[7] S. Schiessl, E. Kucukpinar, S. Cros, O. Miesbauer, H.-C. Langowski, P. Eisner, Nanocomposite coatings based on polyvinyl alcohol and montmorillonite for high-barrier food packaging, Front. Nutr. 9 (2022), https://doi.org/10.3389/fnut.2022.790157.
[8] G. Zehetmeyer, R.M.D. Soares, A. Brandelli, R.S. Mauler, R.V.B. Oliveira, Evaluation of polypropylene/montmorillonite nanocomposites as food packaging material, Polym. Bull. 68 (2012), https://doi.org/10.1007/s00289-012-0722-1. Springer; Springer-Verlag, https://link.springer.com/article/10.1007/s00289-012-0722-1.
[9] H.C. Koh, J.S. Park, M.A. Jeong, H.Y. Hwang, Y.T. Hong, S.Y. Ha, S.Y. Nam, Preparation and gas permeation properties of biodegradable polymer/layered silicate nanocomposite membranes, Desalination 233 (2008), https://doi.org/10.1016/j.desal.2007.09.043.
[10] H. Yang, Z. Shao, W. Wang, X. Ji, C. Li, A composite coating of GO-Al2O3 for tritium permeation barrier, Fusion Eng. Des. 156 (2020), https://doi.org/10.1016/j.fusengdes.2020.111689.
[11] D. Choi, H. Park, J.H. Lim, T.H. Han, J.-S. Park, Three-dimensionally stacked Al2O3/graphene oxide for gas barrier applications, Carbon 125 (2017), https://doi.org/10.1016/j.carbon.2017.09.061.
[12] E.L. Cussler, S.E. Hughes, W.J. Ward, R. Aris, Barrier membranes, J. Membr. Sci. 38 (1988), https://doi.org/10.1016/S0376-7388(00)80877-7.
[13] L.E. Nielsen, Models for the permeability of filled polymer systems, J. Macromol. Sci. Part A - Chemistry 1 (1967), https://doi.org/10.1080/10601326708053745. Taylor & Francis Group.
[14] J. Lommes, G. Patzelt, V. Stenzel, UV-curable polyimide/layered silicate films with improved barrier properties for the protection of semiconductor chips, Microelectron. Eng. 277 (2023), https://doi.org/10.1016/j.mee.2023.112014.
[15] X. Zhang, H. Yi, H. Bai, Y. Zhao, F. Min, S. Song, Correlation of montmorillonite exfoliation with interlayer cations in the preparation of two-dimensional nanosheets, RSC Adv. 7 (2017), https://doi.org/10.1039/C7RA07816A.
[16] J. Lommes, M. Hanf, G. Patzelt, A. Deissenberger, V. Stenzel, A. Hartwig, Freeze drying of organically modified layered silicates as key step to improve the barrier properties of organic coatings for high power electronics protection, Adv. Mater. Interfac. 11 (2024), https://doi.org/10.1002/admi.202300840. John Wiley & Sons, Ltd.
[17] T.T. Zhu, C.H. Zhou, F.B. Kabwe, Q.Q. Wu, C.S. Li, J.R. Zhang, Exfoliation of montmorillonite and related properties of clay/polymer nanocomposites, Appl. Clay Sci. 169 (2019), https://doi.org/10.1016/j.clay.2018.12.006.
[18] J. Lommes, M. Bätcher, A. Deißenberger, V. Stenzel, A. Hartwig, Adjustment of coatings morphology and particle distribution of layered silicates by freeze-drying for improved gas barriers, Adv. Eng. Mater. (2025), https://doi.org/10.1002/adem.202501350.
[19] B. Schartel, U. Knoll, A. Hartwig, D. Pütz, Phosphonium-modified layered silicate epoxy resins nanocomposites and their combinations with ATH and organo-phosphorus fire retardants, Polym. Adv. Techs 17 (2006), https://doi.org/10.1002/pat.686.
[20] T. Aizawa, M. Kubota, T. Ebina, Temperature dependence of gas barrier property of clay-polymer composite coatings, Appl. Clay Sci. 226 (2022), https://doi.org/10.1016/j.clay.2022.106571.
[21] L. Ansaloni, M. Minelli, M. Giacinti Baschetti, G.C. Sarti, Effect of relative humidity and temperature on gas transport in Matrimid®: experimental study and modeling, J. Membr. Sci. 471 (2014), https://doi.org/10.1016/j.memsci.2014.08.019.
[22] G.C. Kapantaidakis, G.H. Koops, High flux polyethersulfone–polyimide blend hollow fiber membranes for gas separation, J. Membr. Sci. 204 (2002), https://doi.org/10.1016/S0376-7388(02)00030-3.
[23] M.C. Celina, A. Quintana, Oxygen diffusivity and permeation through polymers at elevated temperature, Polymer 150 (2018), https://doi.org/10.1016/j.polymer.2018.06.047. Elsevier BV.
[24] G. Mensitieri, M.A. Del Nobile, T. Monetta, L. Nicodemo, F. Bellucci, The effect of film thickness on oxygen sorption and transport in dry and water-saturated Kapton® polyimide, J. Membr. Sci. 89 (1994), https://doi.org/10.1016/0376-7388(93)E0209-3. https://www.sciencedirect.com/science/article/pii/0376738893E02093.
[25] K.A. Stevens, Z.P. Smith, K.L. Gleason, M. Galizia, D.R. Paul, B.D. Freeman, Influence of temperature on gas solubility in thermally rearranged (TR) polymers, J. Membr. Sci. 533 (2017), https://doi.org/10.1016/j.memsci.2017.03.005. https://www.sciencedirect.com/science/article/pii/S0376738816321573.
[26] Z.P. Smith, R.R. Tiwari, T.M. Murphy, D.F. Sanders, K.L. Gleason, D.R. Paul, B. D. Freeman, Hydrogen sorption in polymers for membrane applications, Polymer 54 (2013), https://doi.org/10.1016/j.polymer.2013.04.006. https://www.sciencedirect.com/science/article/pii/S0032386113003200.
[27] G.Q. Chen, C.A. Scholes, G.G. Qiao, S.E. Kentish, Water vapor permeation in polyimide membranes, J. Membr. Sci. 379 (2011), https://doi.org/10.1016/j.memsci.2011.06.023. https://www.sciencedirect.com/science/article/pii/S0376738811004625.
[28] S. Kumar, S. Chattopadhyay, A. Sreejesh, S. Nair, G. Unnikrishnan, G.B. Nando, Analysis of air permeability and WVTR characteristics of highly impermeable novel rubber nanocomposite, Mater. Res. Express 2 (2015), https://doi.org/10.1088/2053-1591/2/2/025001. IOP Publishing, https://iopscience.iop.org/article/10.1088/2053-1591/2/2/025001/meta.
[29] A.G. Erlat, B.-C. Wang, R.J. Spontak, Y. Tropsha, K.D. Mar, D.B. Montgomery, E. A. Vogler, Morphology and gas barrier properties of thin SiO x coatings on polycarbonate: correlations with plasma-enhanced chemical vapor deposition conditions, J. Mater. Res. 15 (2000), https://doi.org/10.1557/JMR.2000.0103. https://www.cambridge.org/core/journals/journal-of-materials-research/article/morphology-and-gas-barrier-properties-of-thin-sioxcoatings-on-polycarbonate-correlations-with-plasmaenhanced-chemical-vapor-deposition-conditions/c4727b3099e0f09cfd581a39f1bd6e5b.